Journal of Drug Delivery Science and Technology 46 (2018) 74–86

Contents lists available at ScienceDirect

Journal of Drug Delivery Science and Technology

journal homepage: www.elsevier.com/locate/jddst

A novel approach for skin infections: Controlled release topical mats of poly (lactic acid)/poly(ethylene succinate) blends containing Voriconazole

Neslihan Üstündağ Okur[a,*], Maria Filippousi[a], Mehmet Evren Okur[b], Şule Ayla[c], Emre Şefik Çağlar[a], Ayşegül Yoltaş[d], Panoraia I. Siafaka[a]

[a] Istanbul Medipol University, School of Pharmacy, Department of Pharmaceutical Technology, Beykoz, 34810, Istanbul, Turkey
[b] Anadolu University, Faculty of Pharmacy, Department of Pharmacology, 26470, Tepebaşı, Eskisehir, Turkey
[c] Istanbul Medipol University, School of Medicine, Department of Histology and Embryology, 34810, Istanbul, Turkey
[d] Ege University, Faculty of Science, Department of Biology, Fundamental and Industrial Microbiology Division, Bornova, 35100, Izmir, Turkey

ARTICLE INFO

Keywords:
Fungal infections
Voriconazole
Topical mat
Dressing
Drug delivery
Antifungal

ABSTRACT

The oral and injectable formulations of Voriconazole (VRZ), a known antifungal agent with low solubility, seem to cause severe side effects. Consequently, topical application of VRZ could be advantageous for skin fungal infections. In this study, VRZ embedded in a polymeric matrix composed of biocompatible poly(lactic acid) (PLA) and poly(ethylene succinate) (PESu). The mats were prepared via solvent evaporation and fully characterized by Fourier-Transformed Infrared Spectroscopy (FTIR), Differential Scanning Calorimetry (DSC), Scanning Electron Microscopy (SEM), *in vitro* hydrolysis and release studies. The prepared blends defined as immiscible by DSC and SEM while FTIR spectroscopy did not disclose noticeable interactions between the polymers. It was found that hydrolysis was improved by increasing PESu content into the blend. VRZ loaded blends spectra exhibit slight differentiation compared to neat blends while the absence of VRZ melting peak, as DSC illustrated, indicated drug amorphization. Lastly, *in vitro* release studies depicted a controlled release pattern dependent on mats' hydrolysis degree. An improved antifungal activity of mats was detected by disc diffusion method against various microorganisms. *Ex vivo* studies of VRZ did not determine high permeation while histopathology results using mice were profitable. The irritation experiments displayed that the mats did not induce any skin irritation.

1. Introduction

Voriconazole (VRZ) [(2R,3S)-2-(2,4-difluorophenyl)-3-(5-fluoropyrimidine-4-yl)-1-(1H-1,2,4-triazole-1-yl)butan-2-ol] is a triazole antifungal agent which is often applied against invasive fungal infections like aspergillosis, candidiasis as well as infections from *Fusarium* species [1–4]. In most cases, fungal infections are found in the skin, the largest human sense organ, whose primary function is to act as a barrier protecting the internal organs from excessive water loss, physical or chemical attack as well as pathogens invasion [5,6]. It has been reported that skin fungal infections such as dermatophytosis and candidiasis, are described as the most common diseases into Asian and African population since they can affect approximately 15% of the population [1,7].

VRZ administration against fungi invasion, either orally or intravenously, is very common due to its favorable safety profile, which is, however, limited by the severe adverse effects such as hepatotoxicity, photophobia, blurred vision as well as photosensitivity etc. In addition, it has been recorded that patients who receive VRZ can present hallucinations and other central nervous system symptoms, such as confusion [8]. Furthermore, it is well reported that azoles during pregnancy are not easily prescribed due to their embryotoxicity and teratogenicity in rodents, rabbits, and rats. In addition, azoles could induce hydronephrosis, reduced ossification as well as fetal mortality. Among others, VRZ possibly can cross the human placenta considering its low molecular weight and so this antifungal agent labeled as category D-fetal risk [9]. In view of such severe toxicity, the topical application of VRZ is required since it could change its limitation and improve its profile.

Topical administration of antifungal agents could have an increased impact on the antifungal therapy, given that current formulations present lack of efficacy due to the rising antifungal drug resistance [10,11]. Although drug administration by skin is very advantageous, it can also be very challenging considering that the skin acts as a barrier to drug transport [12]. Mostly, creams, ointments, oil, and microemulsions are applied such as topical pharmacologic agents because

* Corresponding author.
E-mail address: neslihanustundag@yahoo.com (N. Üstündağ Okur).

https://doi.org/10.1016/j.jddst.2018.05.005
Received 17 February 2018; Received in revised form 3 May 2018; Accepted 5 May 2018
Available online 07 May 2018
1773-2247/

they can penetrate the stratum corneum layer and eliminate fungi (fungicidal agents), or at least inhibit their growing or dichotomy (fungistatic agents) [13]. In the literature, several efforts can be found in order to deliver locally VRZ safely, mostly as ocular drug delivery systems [14–18] or skin delivery systems [19,20]. Nonetheless, the application of a polymeric film as VRZ topical carrier has not been attempted yet.

The last decades, aliphatic polyesters, such as poly(ε-caprolactone)-PCL, poly(lactic acid)-PLA, poly(butylene succinate)-PBSu, poly(lactic acid-*co*-glycolic acid)-PLGA, have gained great attention in pharmaceutical technology as a result of their biodegradability, biocompatibility as well as other physical and chemical properties. PLA, owing to its slow hydrolytic degradation, is one of the most widely used polymer for controlled delivery applications [21–23], tissue engineering [24–26] or implants. An easy method to improve PLA hydrophilicity is to blend it with a more hydrophilic polymer. It has been addressed that blending polymers can result in various release patterns [22,27]. Poly (ethylene succinate)-PESu is a biocompatible polymer with chemical resistance and improved mechanical properties [28]. PLA/PESu blends via solvent evaporation method have been already reported in the literature, nevertheless, have never been applied as drug carriers. In the past study, authors dissolved the homopolymers in chloroform [29] in contrast to our work where dichloromethane (DCM) was applied. Herein, DCM was chosen given its lower toxicity compared to chloroform.

The aim of this work was to introduce an alternative option for topical delivery of VRZ by using PLA/PESu blends in different concentrations. The blends were developed via solvent evaporation technique with dichloromethane as a solvent and studied for their miscibility and compatibility via Fourier Transformed–Infrared spectroscopy, Differential Scanning Calorimetry analysis, and Scanning Electron Microscopy observation. VRZ was added and the prepared mats were also evaluated by these means.

2. Materials and methods

2.1. Materials

Poly(ethylene succinate) and poly(lactic acid) were purchased from Aldrich Chemical Co (Steinheim, Germany). VRZ was also purchased by Aldrich Chemical Co (Steinheim, Germany). High performance liquid chromatography (HPLC) grade Acetonitrile (Sigma, Germany) and Methanol (Sigma, Germany) were used for HPLC studies. All other reagents and solvents used were of analytical grade.

2.2. Topical mats neat and loaded with VRZ preparation via solvent evaporation method

In order to prepare PLA/PESu blends, the solvent evaporation method was used; dichloromethane (DCM) applied as the solvent of the polymeric system. PLA/PESu blends presenting weight ratios 100/0, 90/10, 70/30, 50/50 and 0/100 w/w (mg/mg) were prepared. More specifically, 90 mg of PLA and 10 mg of PESu were used for the preparation of 90/10 blends. In such case, the polymers were dissolved in 5 mL of DCM and left to be fully evaporated. After the complete evaporation, films dried in the oven (25 °C) so as to remove any DCM residues. The mixture was dried up to the point where the mats weight was stable. Similarly, PLA/PESu 70/30 and 50/50 were also prepared. In case of VRZ loaded blends, 5% of VRZ drug loading was achieved. For instance, in case of 90/10 blend 85.5 mg of PLA and 9.5 mg of PESu as well as 5 mg of VRZ was dissolved in DCM and left to fully be evaporated. Afterward, the milk opaque films dried in the oven (25 °C) so as to remove any DCM residues. Accordingly, VRZ loaded 70/30 and 50/50 mats were developed.

2.3. Characterization of the topical mats

2.3.1. Fourier-Transformed Infrared Spectroscopy studies

The prepared mats were studied using FTIR–spectrometer FTIR–2000 (Perkin Elmer, Turkey) so as to record their FT-IR spectra. In order to collect the spectra, a thin film of the prepared 50/50, 70/30 and 90/10 neat and VRZ mats was applied to the spectrometer. The spectrum collection area ranged from 4000 to 400 cm^{-1} with a resolution of 2 cm^{-1} (64 co–added scans). Herein, the presented spectra are baseline corrected and converted to the absorbance mode.

2.3.2. Differential Scanning Calorimetry (DSC)

For thermal analysis, a differential scanning calorimeter (DSC) (Perkin–Elmer, Pyris Diamond, Turkey) calibrated with Indium and Zinc standards, was used. For the characterization, 8 mg of the mats were used, placed in aluminum pans and heated up to 200 °C using a heating rate of 10 °C/min. The mats were held at that temperature for 5 min and then they were cooled down by 300 °C/min rate.

2.3.3. Scanning Electron Microscopy (SEM)

The morphological examination of the VRZ formulations was carried out using a scanning electron microscope (SEM) (Zeiss EVO, USA). The mats were coated with silver so as to obtain a good conductivity of the electron beam. The accelerating voltage was 20 kV, probe current was 45 nA and counting time was 60 s.

2.4. Chemical stability of VRZ mats

The chemical stability of the VRZ mats was calculated at 5 ± 2 °C and 25 ± 2 °C for 12 months. The amount of VRZ was investigated to examine the monthly storage temperature.

2.5. Water uptake and average thickness of the mats

The water uptake was figured out by immersing the mats in distilled water at 25 °C. After 1 h, the hydrated mats were removed, followed by surface water extraction using filter paper and directly weighed. The water content ($W_{H2O\ \%}$) was calculated using the following type ($W_{H2O\ \%}$) = (W-W_o)/W_o % (W_o and W express the mats weight before and after immersion in water, respectively) [30]. The mats thickness was ruled out by a micrometer at random points on the mat surface area.

2.6. In vitro hydrolysis studies of mats

The hydrolysis degree was estimated accordingly with the mass loss. Circular shaped mats with 0.78 cm^2 area were placed in Petri dishes with simulated body fluid (pH 7.4). Afterward, the samples were incubated at 37 ± 1 °C in an oven for a period of five days. Every 48 h, the mats were removed, washed with distilled water, dried and weighted until constant weight [22]. The hydrolysis was calculated using the following formula: % mass loss = (W_1-W_2)/W_2 × 100 (W_1 and W_2 express the mats weight before and after hydrolysis, respectively). All the experiments were performed in triplicate.

2.7. High performance liquid chromatography analysis

For the determination of the drug loading content and *in vitro* release results, HPLC method was applied. The quantitative analysis of the obtained solutions was assessed by HPLC using HP Agilent 1100 system (Germany) consisted of a gradient pump and a UV detector. The used column was a C18 column (5 μm, 150 × 4.6 mm) (GL Sciences, Japan). The samples were analyzed at 256 nm with 1 mL/min at 25 °C flow rate. The mobile phase consisted of Acetonitrile (ACN): ultrapure water (50:50). The retention time of drug was 4.098 min. The method was validated for linearity, limit of detection (LOD) and limit of quantitation (LOQ), precision, accuracy and specificity, selectivity and

stability [31]. The linearity between peak area and concentration was analyzed using calibration curve obtained from standard solutions of VRZ (1–30 μg/mL). The accuracy of an analytical method is the closeness of test results obtained by the method to the true value and is defined recovery. The prepared three standard solutions (8, 11, 14 μg/mL) were injected five times at different levels as a test sample. Eight μg/mL solution was injected ten times in order to evaluate method precision, standard deviation (SD) and coefficient of variation. The Limit of Detection (LOD) and Limit of Quantitation (LOQ) tests for the procedure are performed on samples containing very low concentrations of analytes. If the standard deviation is less than the acceptance criteria which is 2%, the analysis system for the determination of assay is to verify.

2.8. Drug loading content analysis, in vitro drug release and kinetic analysis of PLA/PESu mats

The analysis of the drug loading content was performed with HPLC method as described in section 2.7. Ten mats were grounded separately in a glass pestle mortar and dissolved in 100 ml methanol and mixed with a shaker for 12 h. Then this solution was filtered through the polytetrafluoroethylene (PTFE) membrane (0.45 μm). The average of results was determined. Experiments were performed at 25 ± 2 °C. The drug loading was almost 5% w/w. *In vitro* release study of mats was performed in 10 mL of dissolution medium at 50 rpm. The dissolution medium was 10 mL of a solution simulating the inorganic composition of the body fluids prepared as previously reported [32,33]. The temperature was preserved at 32 ± 0.5 °C to mimic skin temperature. The mats have been shaped 1 × 1 cm^2 (the actual antifungal load is 0.96–1.034 mg/cm^2). 0.5 mL of sample was removed at a predetermined time interval of 30 min–84 h and the same volume of fresh medium was replaced. All measurements were performed in triplicate and herein the mean area is displayed. The data were analyzed via origin pro software.

2.8.1. Kinetic analysis data- model dependent methods

In this study, *in vitro* release results were analyzed using model-dependent methods [34]. Model dependent methods are based on different mathematical functions, which describe the dissolution profile. A computer-based kinetic program provided by Ege and coworkers, as it was previously reported [35,36], was used in order to determine the suitable drug release kinetic model describing the dissolution profile. The large value of the coefficient of determination (r^2) indicated a superiority of the dissolution profile fitting to mathematical models. Numerous models have been conducted so as to determine kinetics of polymeric drug delivery systems [27,37–39] Herein, for the release kinetics examination of the PLA/PESu formulations the following mathematical models were applied:

First order model:

$$Q_t = Q_0 e^{-kt} \quad (1)$$

Zero order model:

$$Q_t = Q_0 + k_0 t \quad (2)$$

Higuchi's model:

$$Q_t = k_H t^{\frac{1}{2}} \quad (3)$$

Korsmeyer—Peppas model:

$$f_t = k_m t^n \quad (4)$$

Hixson-Crowell model:

$$3\sqrt{Q_0} - 3\sqrt{Q_t} = k_{HC} t \quad (5)$$

where f_t represents the fraction of drug dissolved in time t, k_f, k_o, k_H, k_m and k_{HC} are the apparent dissolution rate constants for the first order, zero order, Higuchi model Korsmeyer–Peppas model and Hixson-Crowell model, respectively. In case of Hixson-Crowell, Zero order, First order and Higuchi's model Q_o is the initial amount of drug, Q_t is the cumulative amount of drug release at time t. In case of Korsmeyer-Peppas "n" is the release exponent for Korsmeyer–Peppas model (the value of exponent n is used to characterize the mechanism for both solvent penetration and drug release [40]).

2.9. In vitro cytotoxicity study of PLA/PESu mats

The *in vitro* cytotoxicity of the PLA/PESu mats was evaluated by measuring L-929 fibroblasts viability by the [3-(4,5-dimethylthiazol-2-yl)-2,5-diphenyl tetrazolium bromide] (MTT) assay [33]. L-929 fibroblasts were seeded in 24-well plates at a density of 30.000 cells per well using 200 μL cell culture medium (−90% Dulbecco's Modified Eagle's Medium (DMEM), 10% fetal bovine serum, 1% penicillin-streptomycin solution). Twenty-four hours after plating, various polymer concentrations were added in the wells. After 24 h of incubation at 37 °C, 50 μL of MTT solution (5 mg/mL in PBS pH 7.4) were added into each well and plates were incubated at 37 °C for 2 h. The medium was withdrawn and 100 μL of dimethyl sulfoxide (DMSO) was added to dissolve the formed crystals. The solution was transferred to 96-well plates and immediately read on a microplate reader (Biorad, Hercules, CA, USA), at a wavelength of 540 nm. Biocompatibility of polymers was expressed as % cell viability, which was calculated from the ratio between the number of cells treated with the blends and that of non-treated cells (control). The experiments were performed in triplicate.

2.10. Antifungal activity of the prepared topical PLA/PESu mats

Antifungal activity of PLA/PESu mats against *Candida albicans, Candida tropicalis, Aspergillus flavus, Aspergillus fumigatus,* and *Aspergillus niger* was evaluated using disc diffusion method. Agar well diffusion testing was performed according to CLSI standards. Mueller-Hinton II Agar (Difco) supplemented with 2% glucose and 0.5 μg/mL methylene blue dye (SSI Diagnostica, Hillerød, Denmark) was used. For the moulds (*Aspergillus flavus, Aspergillus niger* and *Aspergillus fumigatus*) inocula were prepared at optical densities ranging from 80 to 82% and a suspension with a 0.5 McFarland standard was utilized for yeasts (*Candida albicans* and *Candida tropicalis*). 100 μL of each suspension were spread evenly onto Mueller-Hinton II Agar using a drigalski spatula and allowed to dry. Wells (diameter = 12 mm) drilled with a sterile corkborer and VRZ disks that were 12 mm in diameter were placed in these wells. The plates were incubated at 35 °C for 24–48 h and inhibition zone (IZs, in millimeters) diameters were read by using a digital ruler at 24 and 48 h. Minor trailing growth in the inhibition zones was ignored. Each test was completed in triplicate and the mean zone size was detected.

2.11. Ex vivo drug permeation study using mice abdominal skin

2.11.1. Preparation of mice abdominal skin

The protocol of the study was approved by Istanbul Medipol University Ethical Committee (approval number 11.10.2017–68). The European Community guidelines as accepted principles for the use of experimental animals were adhered to. BALB-c mice weighing 30 ± 5 g were obtained from the Experimental Animal House of MEDITAM Istanbul Medipol University (Istanbul, Turkey) for *ex vivo* experiments. Mice were kept in a room with a temperature of 22 ± 2 °C with an alternating 12-h light/dark cycle. Afterward, mice were sacrificed with anesthetic ether. The hair of test animals was carefully trimmed with electrical clippers and the full thickness skin was removed from the abdominal region. The skin was washed with water, stored at 4 ± 1 °C overnight and then used for *ex vivo* permeability studies.

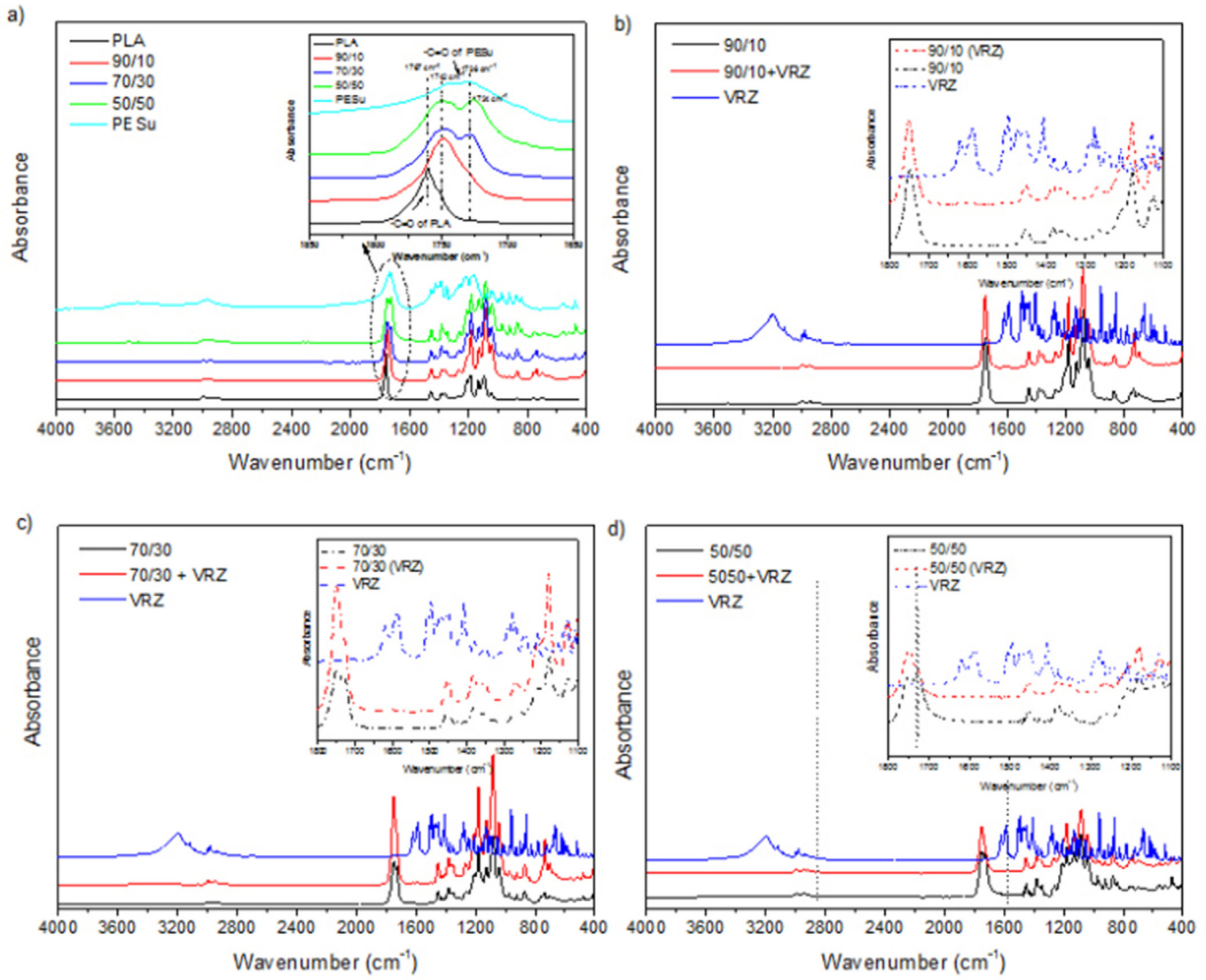

Fig. 1. FTIR spectra of a) PLA/PESu (0/100, 90/10, 70/30, 50/50, 100/0) blends and b) 90/10 neat and loaded with VRZ c) 70/30 neat and loaded with VRZ and d) 50/50 neat and loaded with VRZ (Inset: examination of the region between 1800 and 1100 cm^{-1}).

2.11.2. Penetration and permeation of VRZ loaded PLA/PESu mats

For *ex vivo* permeation study of VRZ loaded PLA/PESu mats, Franz diffusion cells with an effective diffusion area of 0.78 cm^2 were used. The skin was cut into discs and mounted in the Franz diffusion cells. The receiver compartment was consisted of 10 mL PBS/ethanol (80/20, v/v) to ensure sink condition the temperature was maintained at 37 ± 0.5 °C (body temperature) using magnetic stirring at 600 rpm throughout the experiment. Skin sample had the temperature of 32 °C. To prevent evaporation parafilm was applied. For each experiment, 0.1 mL sample of the receiver medium was withdrawn at a predetermined time. The samples were analyzed in HPLC at 256 nm. The cumulative amount (%, w/w) of VRZ permeated through mice abdominal skin was plotted as a function of time. After 24 h of contact time, each skin was washed for penetration study. In further, each skin was cut into minute pieces to determine the amount of VRZ deposited in the skin. They were pooled in a tube containing ethanol, vortexed for 5 min and homogenized to obtain a solution. The obtained solution was homogenized by using homogenizer for 5 min at 26.000 rpm and again vortexed for 5 min and centrifuged for 15 min. Penetrated VRZ (obtained after digestion) was assayed by HPLC study. The cumulative amount penetrating per skin surface area was plotted against time (hours). Experiments were performed in triplicate.

2.12. Skin irritation study

2.12.1. Animals and vivarium housing conditions

It has been addressed that when topical mats are prepared, the safety profile of the formulations should be confirmed. The protocol of the study was approved by Istanbul Medipol University Ethical Committee (approval number 11.10.2017–68). The European Community guidelines as accepted principles for the use of experimental animals were adhered to. For skin irritation experiment healthy BALB-c mice were used. Mice were kept in a room at 22 ± 2 °C with rotating 12-h light/dark cycle. Mice had free contact with food and water ad libitum. The mice were carried to a laboratory 1 h before the test activated. All tests were completed between 09:00 and 12:00 h in normal room light and temperature (22 ± 1 °C). Mice were divided into three groups of four animals each:

Group I: PLA/PESu (70/30) + VRZ mat group,
Group II: PLA/PESu (50/50) + VRZ mat group,
Group III: Control group (serum physiologic, (SP)).

Dorsal skin was shaved before the experiment using a razor with no apparent cuts or injuries. Mats and SP were topically applied to mice

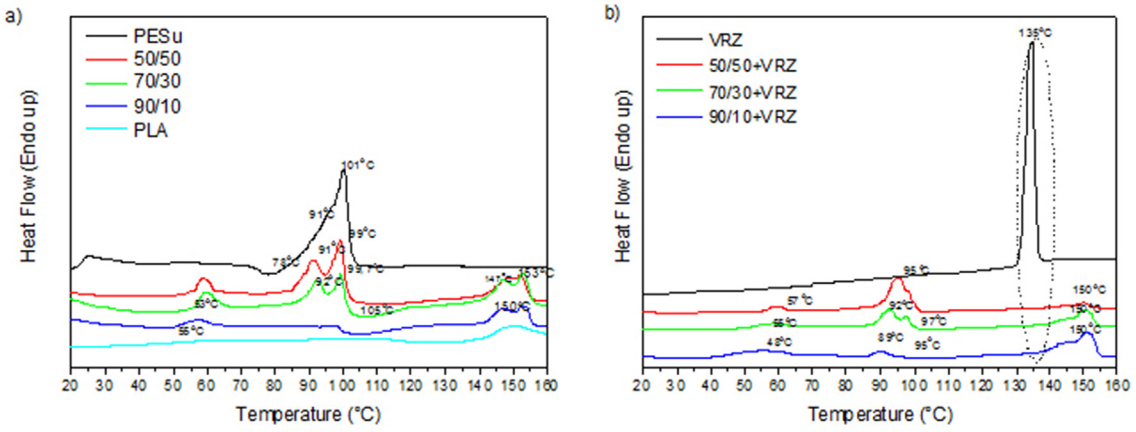

Fig. 2. DSC thermograms of PLA/PESu (100/0, 90/10, 70/30, 50/50 and 0/100) blend a) neat and b) loaded with VRZ.

dorsal skin for 24 h. After 24 h, mice were sacrificed with anesthetic ether.

2.12.2. Histopathology examination

The skin was excised from the dorsal and the subcutaneous fat and connective tissue were trimmed. The skins were wiped off with tissue paper and fixed in formalin solution 10% in saline for one day; afterward washed with water, dehydrated with ethanol, immersed in xylene and were lastly embedded in paraffin wax at 56 °C. Paraffin blocks were cut at 5 μm with a rotary microtome. Sections were stained with Hematoxylene & Eosine and examined using the light microscope (Nikon Eclipse Ni research microscope).

2.13. Statistical analysis

All statistical analyses and graphs were performed using Origin Pro and GraphPad Prism 7.0 software program. The results were expressed as means ± standard deviation (SD). Statistical significance between groups was analyzed by one-way ANOVA followed by Dunnett's post hoc test. Values for $p < 0.05$ were considered statistically significant.

3. Results and discussion

3.1. Miscibility and compatibility studies of the prepared mats; FT-IR spectroscopy, thermal analysis and morphology observation (SEM)

3.1.1. FT-IR spectroscopy of the prepared PLA/PESu mats

The most important outcome when new formulations are prepared and studied is to identify the evolved interactions, which are taking place between the molecules and polymers. These interactions can result in drug amorphization and different dissolution properties. All the more when polymeric blends are used as such carriers, these interactions could lead to new products miscible, immiscible or partially miscible blends. Generally, PLA blends with other aliphatic polyesters never lead to miscible systems, considering that interactions between PLA and polyesteric domains are weak or nonexistent [22,29]. Even though PLA and PESu blends have been prepared, in the past, herein is the first attempt of such blends to be applied as pharmaceutical formulations.

FT-IR spectra of the prepared PLA/PESu blends are presented in Fig. 1a. As it was expected, PLA spectrum exhibited the characteristic bands associated with the stretching ester carbonyl groups vibration of 1767 cm^{-1}. In case of PESu, two peaks of 1742 and 1736 cm^{-1} are observed linked with the PESu absorbance in amorphous and crystalline domains, respectively [29]. Moreover, when the prepared PLA/PESu blends are studied the characteristic carbonyl group has shifted in lower wavenumbers closely to PESu. Mostly, such shifting indicates interactions between the initial homopolymers. However, in case of aliphatic polyesters, it cannot safely be concluded that interactions are taking place [22,27]. Subsequently, the absence of interactions between the two components indicates that the mixtures are immiscible [27]. In order to reinforce our statement of immiscibility as FT-IR revealed, DSC studies were conducted. Further, it should be noted that the prepared blends were opaque and had a milk-white color indicating that the polymers were crystallized when they blended.

FT-IR spectroscopy studies for PLA/PESu mats loaded with VRZ are seen in Fig. 1 b, c, and d. VRZ spectrum displayed a broad peak of hydroxyl groups and aromatic rings at 3200 and 3121 cm^{-1}, respectively. Peaks at 1615 and 1586 cm^{-1} are correlated with aromatic C–C stretch while sharp peaks from 690 to 515 are due to the Fluoro group presence. In addition, at 665 cm^{-1} N(2), N(4), coordination mode of 1H, 1,2,4-triazole is depicted whereas 1007 cm^{-1} is attributed to C–F stretching. In further, C-O stretching mode is seen at 1277 cm^{-1} and C=N stretching is found at 1620 cm^{-1}. Moreover, CH_3 bending adsorption is found at 1277 cm^{-1} [1,12,17,41].

It has been already reported that aliphatic polyesters, when applied as carriers, did not provide any interactions between the polymers and the drugs [22]. Accordingly, when VRZ was incorporated to the PLA/PESu mats, some bands shifted in lower wavenumbers while two new peaks assigned to VRZ drug at 1619 and 1592 cm^{-1} attributed to aromatic C–C stretch can be seen. This observation indicated the successful drug loading. Regularly, if some characteristic bands of the polymer are shifted could exhibit interactions between drug and carriers [22,27]. Nonetheless, this shifting is not so significant to safely presume possible evolved interactions [27].

3.1.2. Thermal analysis of the prepared PLA/PESu mats via Differential Scanning Calorimetry

It is well known that the miscibility or immiscibility of polymer blends as drug delivery carriers could differentiate drug release pattern [22,27]. Among others, it is well understood that polymer blends miscibility, is established by the presence of one single phase. Considering this, only one melting point (T_m) or one glass transition temperature (Tg) should be depicted in DSC thermograms. This temperature is mostly found between the temperatures of the initial polymers, or at even higher temperatures [22,27]. In Fig. 2a–b, DSC thermograms of neat polymers (PLA and PESu), pure PLA/PESu blends and blends with VRZ are shown. From Fig. 2a, it can be confirmed that PLA is a semicrystalline polymer with a Tg value at 55 °C and a T_m at 150 °C [22,42].

In detail, in case of PESu, one melting endotherm (101 °C) with one shoulder (91 °C) and a crystallization exotherm (78 °C) just prior to the melting endotherm is seen. In a previous study, this crystallization exotherm is ascribed to the melt recrystallization of crystallites melting

with low thermal stability. Moreover, the observed shoulder was considered as the melting endotherm of the crystallites with high thermal stability, while the final melting endotherm is associated with the melting of the crystallites formed through the organization of the crystallites with high thermal stability during the DSC heating [28]. In case of 90/10 w/w blend presents a possible miscibility since PESu melting point is not recorded. Nevertheless, it is possible that PESu concentration is low and thus cannot be observed [22,27].

Furthermore, when 70/30 w/w blend is studied, the melting point of PESu is recorded at 99 °C with a shoulder at 91 °C as well as T_m of PLA is found at 153 °C with a shoulder at 147 °C (Fig. 2a). Similar results are found in case of 50/50w/w blend. Accordingly, it can be concluded that the blends comprised from 30 to 50 wt% PESu are immiscible, probably because PESu crystallized in the amorphous PLA matrix.

Fig. 2b shows pure VRZ and VRZ loaded PLA/PESu blends. As it can be ascribed, VRZ is a highly crystalline drug with a melting point at 133 °C which is in accordance with the literature reported melting temperature [43]. In most cases, solvent evaporation can lead to full amorphization of an active molecule or the fine dispersion of the drug into the polymeric solution can also induce such amorphization [22,27]. In this study, DSC thermograms of PLA/PESu blends loaded with VRZ demonstrated drug amorphous dispersion into the matrix due to the lack of VRZ melting point given that only T_m and Tg of the polymers is recorded, similarly to the unloaded mats [1,22,27] (Fig. 2b). Needless to say, that this amorphous dispersion played a role in the better dissolution characteristics of the drug.

In detail, in case of PLA/PESu - 90/10 blend the melting point of PESu is recorded at 95 °C with the shoulder to appear at 89 °C whereas T_m of PLA is found at 151 °C with a shoulder at 142 °C. The Tg of PLA was slightly decreased at 48 °C from 55 °C. Similarly, when PLA/PESu - 70/30 blend studied the melting point of PESu is recorded at 97 °C with the shoulder to appear at 92 °C whereas T_m of PLA is found at 151 °C with a shoulder at 143 °C and the Tg of PLA was found at 55 °C. Finally, PLA/PESu - 50/50 blend depicted the melting point of PESu at 98 °C with the shoulder to appear at 95 °C while T_m of PLA is found at 151 °C with a shoulder at 143 °C. Herein, Tg of PLA was almost similar with the neat 50/50 blend. It can be concluded that Tg, as well as Tm values of the polymeric components, are decreasing due to the VRZ presence. This fact attributes that VRZ drug enacts as a plasticizer in the system, as it has been summarized in past studies [22].

3.1.3. Morphology observation with Scanning Electron Microscopy (SEM)

In general, the morphology of polymeric blends is altered by various parameters like the nature of the polymers, the composition of the blend as well as the processing methods. Several optical methods have been used so as to study the morphology of immiscible or incompatible blends; Scanning Electron Microscopy belongs to such techniques.

Preliminary observation of the blends exhibits structurally uniformity while the thin PLA/PESu films had an opaque white milky color, which also implies that PLA/PESu mats are immiscible and have separated phases [27]. In further, SEM micrographs of blends (Fig. 3a, b, c) also depicted the low miscibility between the two polymers since different phases were observed [27]. This finding is presumed since the surface is not smooth, presenting PESu phase dispersed into the PLA matrix. The PESu phase appears in the micrographs as empty spaces scattered throughout the PLA matrix.

3.2. In vitro cytocompatibility, average thickness, water uptake, chemical stability and in vitro release studies of VRZ loaded mats

Firstly, in order to determine the safety of the prepared mats for skin application, *in vitro* cytocompatibility of PLA/PESu mats was examined using L-929 fibroblasts [22,33]. As it can be obvious from Fig. 4, the mats present high cell viability and thus can be further applied as topical mats. This high cell viability was rational given that both materials are used in pharmaceutical and tissue engineering applications due to their relatively low toxicity.

Among other parameters, thickness and moisture uptake are also significant when topical mats are developed. In this study, although both PLA and PESu are hydrophobic materials, their blends absorbed water as Fig. 5 showed. Most specifically, by increasing PESu content the water uptake also increased; in case of PLA 0% water was absorbed but for 90/10, 70/30 and 50/50 water uptake was found at 8,88%, 11,4 and 25,9%, respectively. This presence of the water in the matrix can be linked with the porosity as it was found from SEM micrographs (Fig. 3a, b, c). Similar results were also reported for hydrophobic fibrous blends due to their porosity [22].

Additionally, chemical stability of VRZ in the mats was also determined and found to be sufficient at 5 ± 1 °C and 25 ± 2 °C whereas the drug entrapment was relatively high ranging from 92 to 100%. Drug loading content was calculated as 5% w/w. Finally, the average thickness of the prepared mats found between 0.09 and 0.1 mm. To summarize, all mats displayed similar thickness and water uptake, which is quite advantageous and thus solvent evaporation, can be further used as an easy method to prepare topical mats with similar characteristics.

As it has already been stated, VRZ categorized as class II on biopharmaceutics classification system in view of its low aqueous solubility. In this study, this problem overcame by incorporating VRZ into PLA/PESu blends. By reviewing drug delivery literature, the release rate is associated with several factors such as amorphization and hydrolysis rate. Obviously, hydrolysis is produced more rapidly in the amorphous state while the drug can be diffused more quickly in rubber state than glassy state [22,27,44]. It has also been referred that immiscible blends show an immediate release since free channels are performed, leading to higher release rates [22,27]. In addition to this, blending less hydrophobic polymers with high hydrophobic polymers leads to improved hydrolysis rate. In this work, *in vitro* drug release studies are seen in Fig. 6. In case of neat PLA loaded with VRZ, it can be concluded that the drug was dissolved at almost 5% in 80 h. This is rational considering that PLA is favorable to control release and slow the dissolution [22,45].

Additionally, PLA cannot be fully degraded under simulated conditions [22] as Fig. 6a showed. Similar behavior is found for 90/10 film with a slightly higher release in 80 h. It can be further referred that the addition of PESu seems to improve the release accordingly with hydrolysis degree. Moreover, 70/30 blends released the drug quicker and about 40% of the drug is dissolved in 80 h. These blends present a steady and controlled dissolution pattern as result of the higher degree of PESu in the blend.

Finally, different behavior is indicated for 50/50 blend, which presents the highest degree of hydrolysis (Fig. 6a) in 5 days (almost similar to PESu hydrolysis). Proportionately, the same blend completely releases VRZ in 80 h (Fig. 5b). This can be explained by two factors a) the amorphization of drug and b) the higher hydrolysis rate. More specifically, the mechanism of VRZ dissolution from 50/50 blend is differentiated compared to the other blends. From 0 to 4 h only 10% of the drug is dissolved, however, with the passage of the time VRZ is released more quickly. For example, from 0 to 36 h almost the 65% of the drug is dissolved. Further investigation revealed that from 36 h till 84 h almost 100% of the drug was released.

3.2.1. Kinetic analysis

Evidently, drug release processes include drug dissolution, diffusion through the polymeric matrix, eventually polymer swelling or erosion as well as drug transfer to the receptor solution. Researchers can imply mathematical models only in case of which involved phenomena have been conclusively proved.

Several models can be applied to study the drug release kinetics from polymeric matrices. The most used are zero and first order model, Higuchi, Hixson, and Crowell model as well as Korsmeyer- Peppas

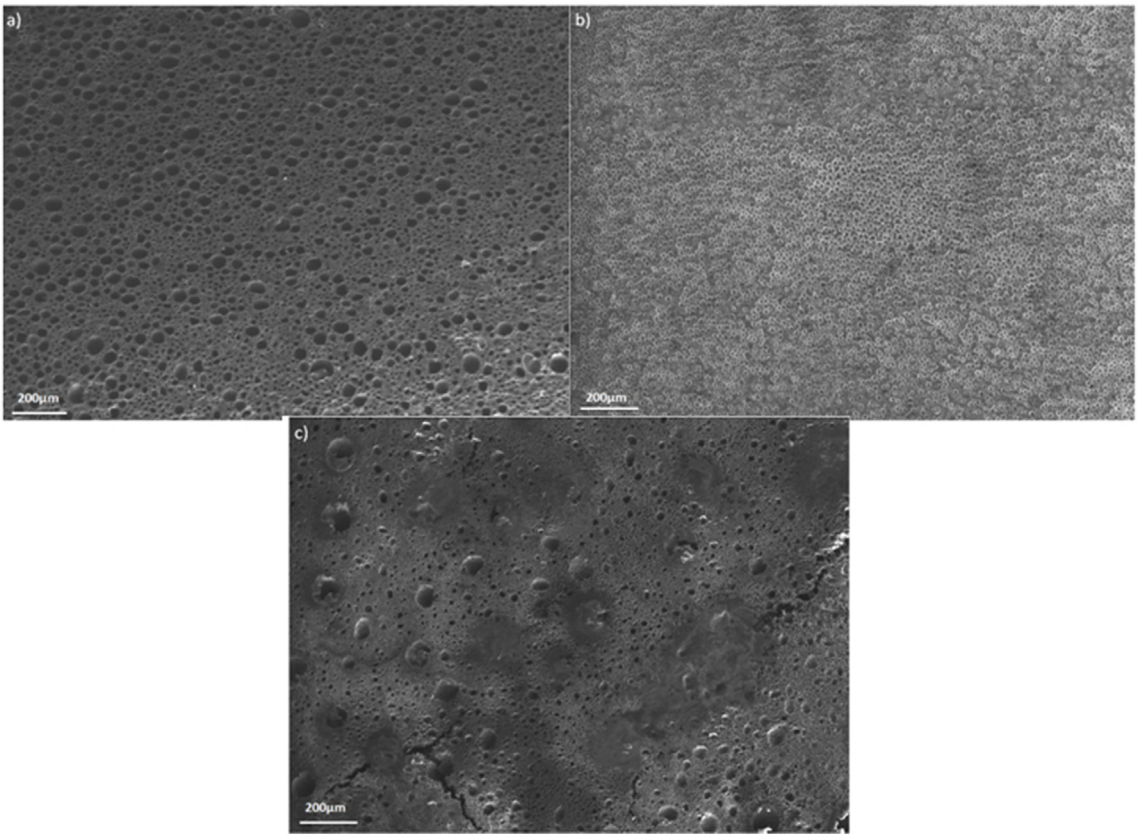

Fig. 3. SEM micrographs of PLA/PESu w/w a) 90/10 (original magnification value × 150), b) 70/30 (original magnification value × 200) and c) 50/50 (original magnification value × 100) blends.

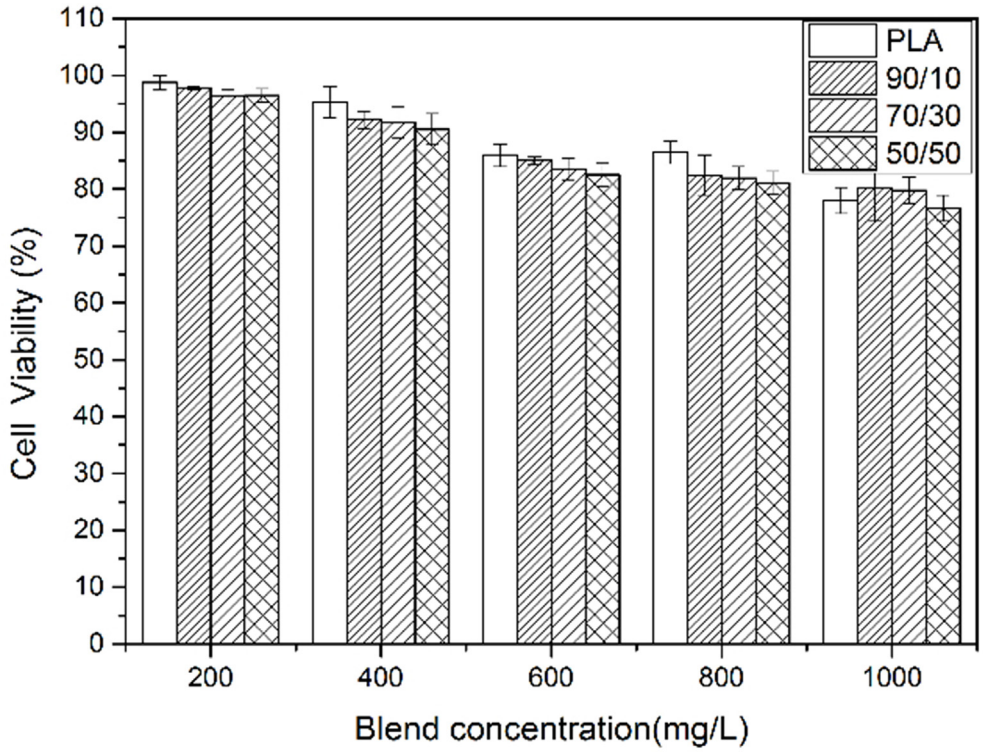

Fig. 4. *In vitro* cytocompatibility of PLA/PESu (100/0, 90/10, 70/30 and 50/50) blends.

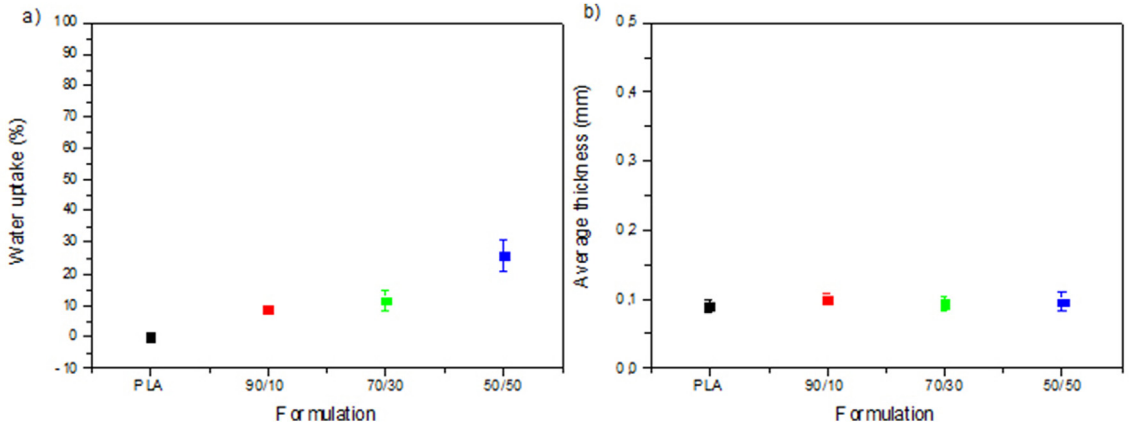

Fig. 5. a) Water uptake and b) Average thickness of the prepared PLA/PESu (100/0, 90/10, 70/30 and 50/50) mats.

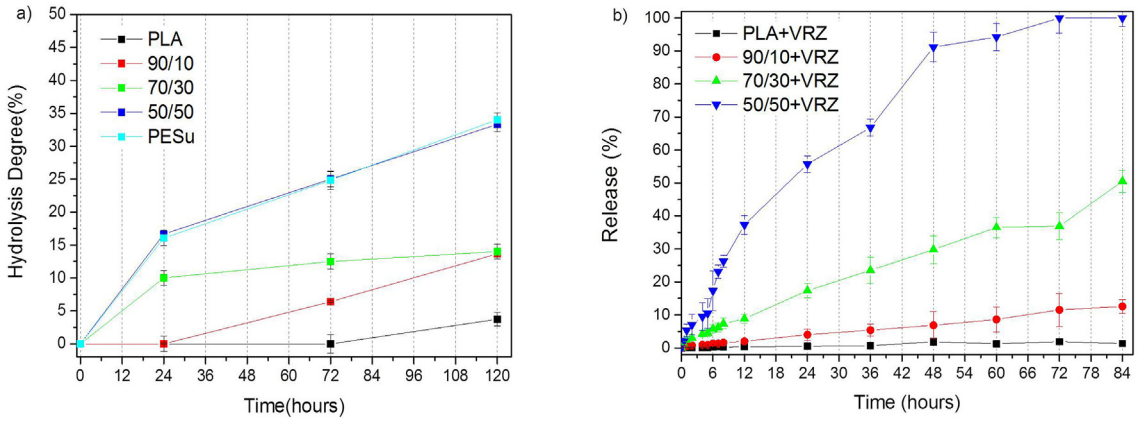

Fig. 6. a) Hydrolysis studies and b) *In vitro* VRZ drug release of 50/50, 70/30 and 90/10 PLA/PESu mats (n:3).

Table 1
Kinetic data of VRZ release parameters obtained from VRZ loaded mats.

Models	Zero order			First order			Higuchi			Hixson-Crowell			Korsmeyer-Peppas	
Mats	r^2	n	m	r^2	n	m	r^2	n	m	r^2	n	m	r^2	n
90/10 + VRZ	0.9956	0.3591	0.0024	0.9943	4.6022	−0.00	0.9467	−1.8936	0.1824	0.9948	0.0049	0.00	0.9797	1.131
70/30 + VRZ	0.9883	2.2977	0.0092	0.9802	4.5943	−0.0001	0.9641	−6.5285	0.7006	0.9850	0.0242	0.0002	0.9865	0.720
50/50 + VRZ	0.9685	6.0625	0.0303	0.9310	4.6728	−0.0007	0.9742	−14.0057	1.8366	0.9696	−0.001	0.0008	0.9757	0.7603

Table 2
Inhibition zone diameters (mm) of blank and VRZ loaded PLA/PESu mats against several types of microorganisms (*Candida albicans, Candida tropicalis, Aspergillus flavus, Aspergillus fumigates, Aspergillus terreus*, *Aspergillus niger*).

Formulations	Microorganisms					
	Candida albicans	*Candida tropicalis*	*Aspergillus flavus*	*Aspergillus fumigatus*	*Aspergillus terreus*	*Aspergillus niger*
PLA	0	0	0	0	0	0
90/10	0	0	0	0	0	0
70/30	0	0	0	0	0	0
50/50	0	0	0	0	0	0
PLA + VRZ	33.5–34.5	49–49	47–49	44–47.5	45–47	47–47
90/10 + VRZ	23–25	45.5–46.5	55–55	51–51	53–59	55–57
70/30 + VRZ	10–12	55–55	64–64	54–53.5	62–62	62–68
50/50 + VRZ	28–32	56–60	74–76	66–68	63–67	70–70
Control	23–25	57–58	73–75	68–69	75–76	74–75

model. In some cases, the release is driven by swelling or erosion of the polymer whereas in other cases the diffusion and dissolution of the drug could play the major role. In general, different mechanisms can be happening at the same time or in stages during the release process. It seems to be highly important to establish which mechanism drives the release in order to successfully design and manufacture the controlled release systems and to identify potential failure modes [46].

In this work, it was assumed that the prepared PLA/PESu

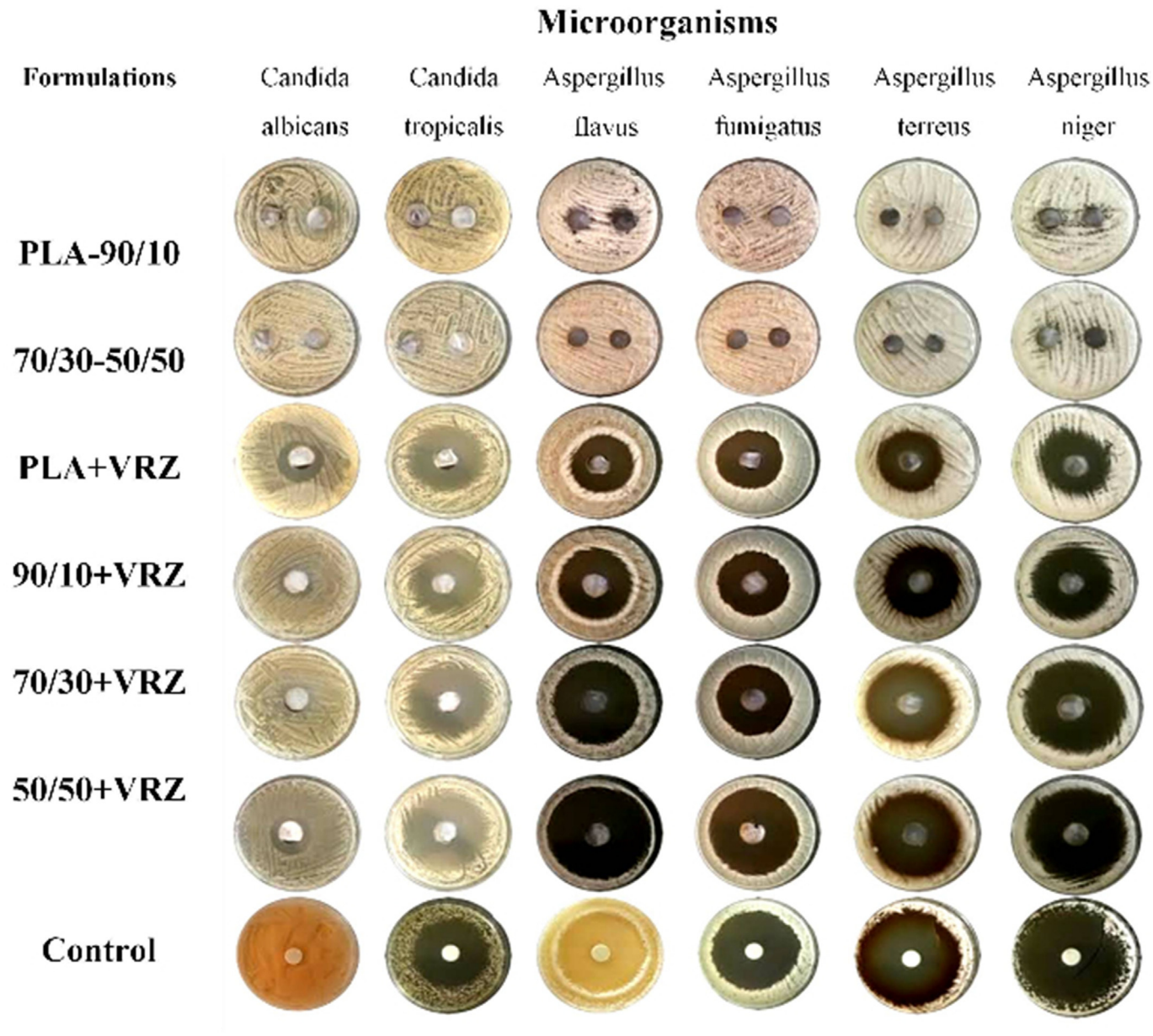

Fig. 7. Antifungal activity of the blank and VRZ loaded PLA/PESu (90/10, 70/30 and 50/50) blends.

formulations loaded with the lipophilic VRZ are diffusion controlled systems since similar studies exhibit accordingly results.

The data from *in vitro* release studies of 90/10 + VRZ, 70/30 + VRZ and 50/50 + VRZ mats were evaluated according to the zero order, first order, Higuchi, Hixson Crowell and Korsmeyer-Peppas kinetic models (Table 1). It was believed that release mechanism herein is not due to swelling or erosion in case of 90/10 loaded with VRZ mats since hydrolysis was negligible. As it was expected, for 90/10 + VRZ, release data were fitted to the zero order followed by Hixson Crowell model. Consequently, dissolution of VRZ molecule is only a function of time.

For 70/30 + VRZ both zero order and Hixson Crowell models could be both applied because the r^2 values were very close to each other as 0.988 and 0.985, respectively (Table 1). Therefore, it can be concluded that these mats ensure a controlled release mechanism. In similar manner, a hydrophobic drug from PLGA nanoparticles also fitted to zero-order model [47]. In another study, Frederikse et al. prepared polymeric films and evaluated *in vitro* release of betamethasone 17-valerate from polymeric films. The betamethasone 17-valerate release data fitted to zero-order kinetics [48].

It was made an assumption that in case of 50/50 + VRZ mats due to higher hydrolysis rate of the neat blend an erosion of the polymer would have affected the release mechanism. It was found that the R^2 value is higher for Higuchi's model compared to Hixson Crowell and zero order models identifying that VRZ release from 50/50 + VRZ mats followed diffusion rate controlled mechanism. Chantasart et al. develop and characterize the prolonged release piroxicam transdermal patch. Drug release kinetic data from the films fitted with the Higuchi model, and the piroxicam release mechanism was diffusion controlled [49].

Furthermore, *in vitro* release kinetics of VRZ loaded mats were also examined by the Korsmeyer-Peppas model. From models characteristics, when $n = 1$, the release rate is independent of time (zero-order) (case II transport); $n = 0.5$ is for fickian diffusion; and $0.5 < n < 1.0$, means diffusion and non-fickian transport are implicated. Lastly, when $n > 1.0$ super case II transport is apparent 'n' is the slope value of log $mt/m\infty$ versus log time curve [50]. The n values of Korsmeyer-Peppas model of the mats were determined as 1.13, 0.720 and 0.760 for 90/10 + VRZ, 70/30 + VRZ and 50/50 + VRZ, respectively. The n values

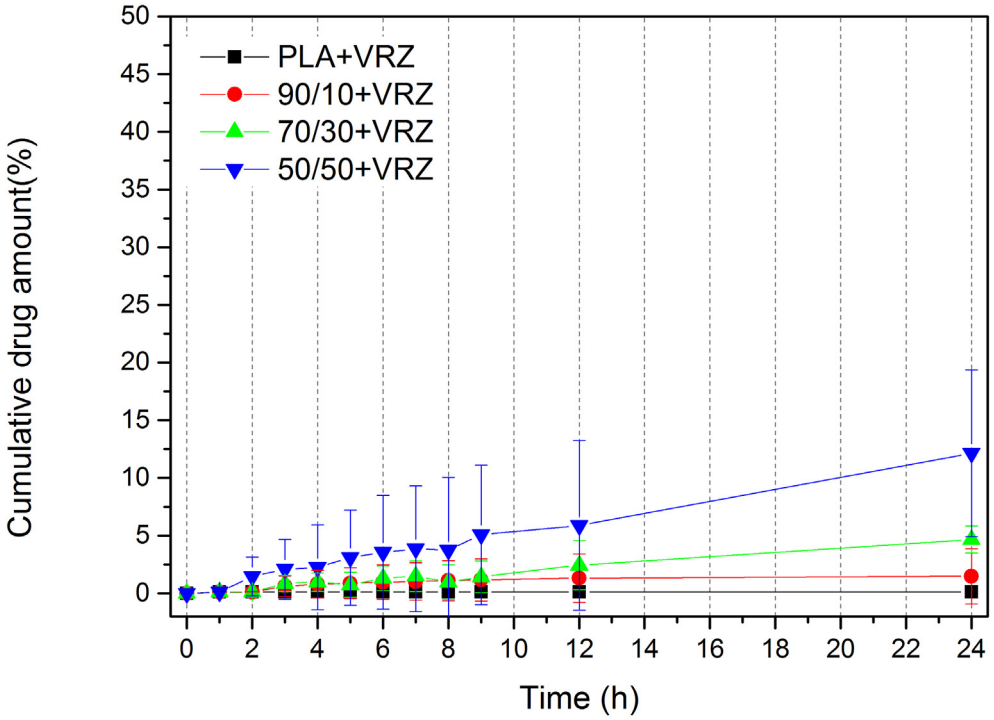

Fig. 8. Cumulative permeation of VRZ through excised mice skin from PLA/PESu (90/10, 70/30 and 50/50) loaded mats (n:3).

(0.720 and 0.760) of 70/30 + VRZ and 50/50 + VRZ mats are not compatible with the Fick's law and release mechanism of these films was determined as diffusion and polymer erosion to a controlled release with relaxation (Table 1). Similarly, fibrous blends of PLA/PBAd and PCL/PPGLu blends loaded with hydrophobic drugs were also fitted to Korsmeyer-Peppas model [22,27].

3.3. Antifungal activity of the PLA/PESu prepared mats

The antifungal activity of the mats was tested against various pathogens such as *Candida albicans*, *Candida tropicalis*, *Aspergillus flavus*, *Aspergillus fumigatus*, *Aspergillus terreus* and *Aspergillus niger* by disc diffusion method. The above species were chosen as they are the most common pathogen causing fungal infections.

In particular, although yeasts are not naturally pathogenic, the alteration of the host's cellular defenses, normal flora or function of the skin, can lead to colonization, infection, and disease. *Candida* species are normally found on the oropharynx, gastrointestinal tract, and vagina. However, moisture and wet conditions help *Candida* to overgrowth and so superficial infections of the skin could also happen. *Candida albicans* is the most virulent of the species causing nails, skin, mucous membranes and viscera diseases [51]. Furthermore, *Candida albicans* have been isolated from biofilms which formed on implanted medical devices or on human tissue [52]. Moreover, *Candida tropicalis* species are less common in causing human disease. In a past study, *Candida tropicalis* species depicted negligible adherence to epidermal corneocytes and were found nonpathogenic to skin however such species are occasionally systemic pathogens associated with septicemia [53]. In addition to this, *Candida tropicalis* was found mostly in nosocomial infections as well as immune compromised patients [54].

Aspergillosis is typically occurred by the inhalation of the fungal spores, which are entry of the pathogen into the body, and the organism has a predilection for the respiratory tract. On the contrary, primary cutaneous infection with *Aspergillus* as well as onychomycosis or otomycosis could also happen [55]. In most cases, *Aspergillus* colonization of burn eschars and traumas is common mostly in immunocompetent patients. In primary cutaneous aspergillosis, typically can be found fungus implantation on the trauma site, including infections of intravenous cannulas, or venipuncture wounds, especially for those who covered with dressings [56].

Considering the above statements, antifungal studies of topical mats against such pathogens are highly significant. From the results (Table 2 and Fig. 7) VRZ loaded formulations present major antifungal properties. More particularly, the VRZ loaded formulations have high fungistatic results and high inhibition zones. Given that the zone diameters are increased as PESu content is increasing, it can be summarized that antifungal properties are proportionally equivalent to *in vitro* release studies. In further, comparing the two studied *Candida* species, *C. albicans* and *C. tropicalis*, it is appeared that *tropicalis* spp are more susceptible to VRZ than *albicans* spp. Nonetheless, the difference is not of great importance. Among others, *Candida* spp compared to *Aspergillus* spp are less sensitive to VRZ. Finally, the comparison between *Aspergillus* spp, showed that *Aspergillus flavus* present the higher inhibition. Finally, it can be summarized that the developed novel formulations can be applied effectively as antifungal agents, given that the studied microorganisms are commonly found in skin fungal infections.

3.4. Ex vivo penetration and permeation of VRZ mats

The assessment of percutaneous permeation of active molecules plays a crucial role during the examination of the dermal or transdermal systems, especially when the drugs would be applied for human's delivery. In most cases, *in vivo* human studies are the best solution, however, due to several reasons, these studies are not easily getting done. Instead of human skin examination, several models have been developed such as *ex vivo* human skin, *ex vivo* animal skin or artificial skin models. Mice and rat skin belong to the most used models [57].

Ex vivo drug penetration and permeation studies using diffusion cells were conducted to investigate the release of drug and predict *in vivo* performance of VRZ. The permeation profile of VRZ through mice skin is seen in Fig. 8 exhibiting a steady increment of VRZ in the receptor chambers over the time. More specifically, after 24 h of the contact period, 50/50 blends permeation was detected as nearly 10% in

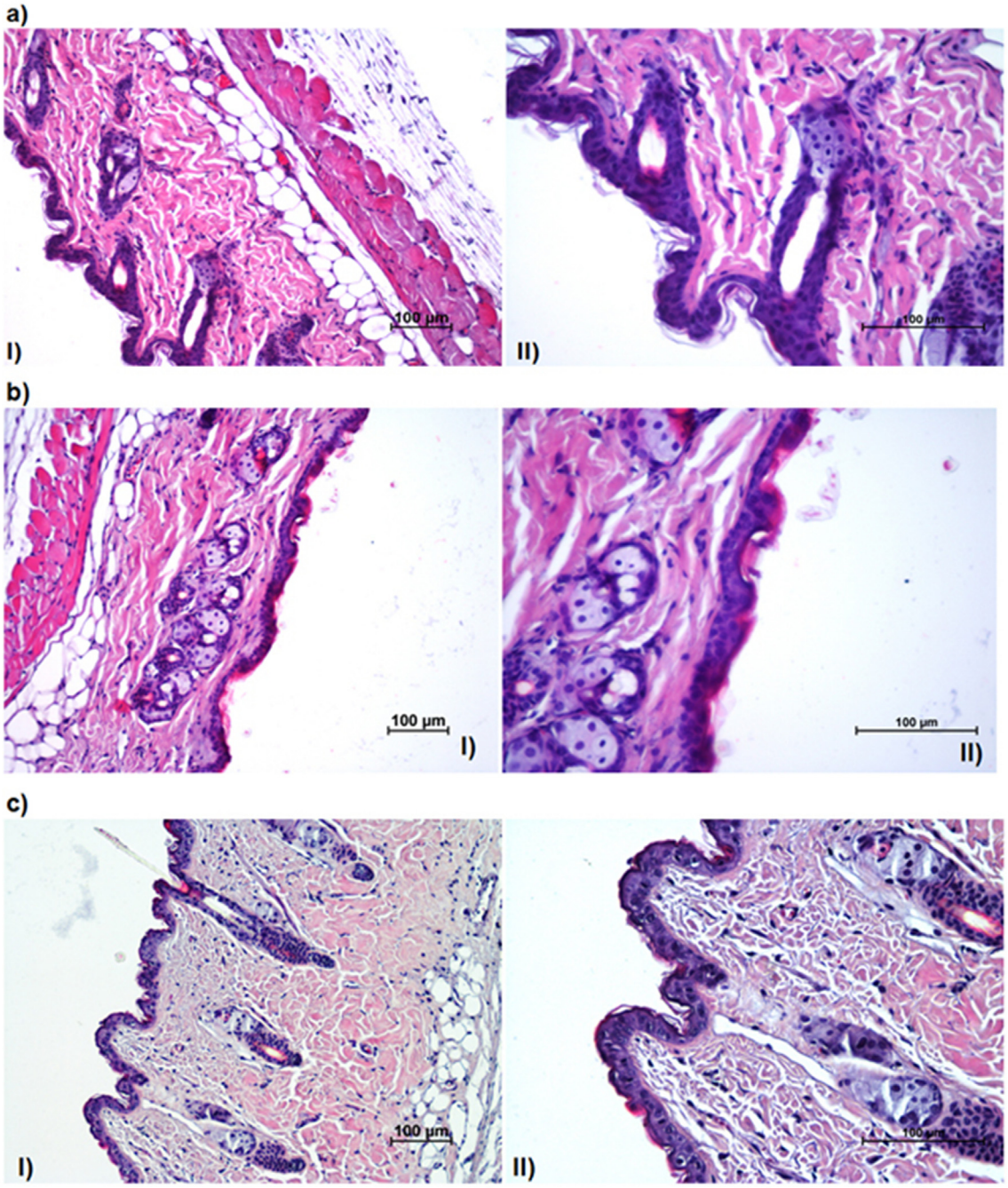

Fig. 9. Images of treated mice skin with a) PLA/PESu (70/30) + VRZ, b) with PLA/PESu (50/50) + VRZ and c) with SP. I: 20× (magnification value), II: 40×, H&E (Hematoxylene and Eosin).

the receptor compartment. In case of VRZ permeation from PLA and 90/10 was detected after 24 h relatively low as 0,13 and 1,4843%, respectively. In comparison to PLA and 90/10 blends, 50/50 blends had statistically significant permeation values ($P < 0.05$). VRZ permeation from 70/30 mats was determined 4.6%. Consequently, a higher permeability of VRZ through the skin is associated with the presence of PESu in the mats. Nonetheless, the low permeation of the drug is rational given that the prepared mats are solid and it is well known that the release is dependent on the swelling ability of the formulation and drug diffusion [50].

When the penetration to the skin tissue was examined, it was ruled out that 70/30 (0.24%) and 50/50 (1.62%) mats obtained higher penetrated VRZ amount than PLA (0.05%) and 90/10 (0.07%) mats. As it was expected, 50/50 mats had higher permeation and penetration values compared to the other mats. The mats did not penetrate any statistically important drug amount to the skin tissue ($P > 0.05$). However, the penetration and permeation values are relatively negligible. Considering the results, the prepared mats could be safely applied as systems for topical delivery of VRZ. These topical mats will be effective for cases such as pregnant patients or children since drug side effects will be limited. Thus, the developed PLA/PESu mats loaded with VRZ offer a safer and promising solution in fungal infection management [58].

3.5. Skin irritation test via histopathology studies

When new topical mats are developed, skin irritation test should be performed and evaluated to conclude that the mats are safe to be used.

As it has been already found out (Fig. 4.) the prepared mats found biocompatible when fibroblasts cultures were used. In order to reinforce this statement, histopathology studies were also performed by using Balb-c mice.

Throughout literature, several animal models have been researched in order to study fungal infections. In most cases, laboratory mice are most commonly used to model clinical syndromes associated with pathogenic fungi whereas also rats, guinea pigs, rabbits, and zebrafish have also been applied. Balb-c mice model can be found in the literature as useful to study fungal infections [59], dermal toxicity as well as eczema or skin lesions study [60–62] as part of preclinical studies.

For the test, 70/30 + VRZ and 50/50 + VRZ were chosen since they showed higher penetration of drug; thus, the safety of these mats should be determined. The influence of the mats on skin irritation was examined by topically applying the film. Microscopic images of mice dorsal skin treated with the mats (70/30 + VRZ and 50/50 + VRZ) and SP are shown in Fig. 9. Disruption degrees of epidermal layers and inflammation degrees of dermal layers were evaluated as weak, moderate and severe for chosen drug loaded formulations and control group. There was only a moderate disruption on the stratum corneum and no disruption on the other epidermal layers whereas no inflammation was observed on the dermal layers.

As it can be observed the stratum corneum layer turned thinner after application of the mats; nevertheless, it is not observed any visible difference in skin morphology (other skin layers and dermis) after 24 h application of 70/30 + VRZ and 50/50 + VRZ. Additionally, erythemas were not observed in any animal after topical application of the mats. The dermis and epidermis layers evaluated as normal, similarly to SP application (Fig. 9c). In comparison to the negative control, the mats have not caused any statistically important histopathological changes on the skin ($P > 0.05$). In further, the irritation experiments have not displayed noticeable irritation, 24 h after when 70/30 + VRZ (Fig. 9a) and 50/50 + VRZ (Fig. 9b) mats applied on the dorsal skin of mice. When SP (negative control) applied, also no inflammation in the dermal layers and no damage in the epidermal layers were seen in the skin. Nonetheless, it should be reported that in case of 70/30 and 50/50 mats, a moderate damage was detected in the stratum corneum which is acceptable given that SC consists of dead cells (corneocytes) and fungi are mostly colonized in SC layer [63].

4. Conclusion

VRZ loaded topical mats composed of PLA and PESu in different concentrations were successfully prepared via solvent evaporation method in order to be used against fungal infections. The prepared mats of the two aliphatic polyesters were determined as immiscible blends as FT-IR and DSC studies indicated. DSC studies illustrated amorphization of VRZ into the matrix. Interactions between VRZ and the carriers were not signified by FT-IR studies. Degree of hydrolysis and *in vitro* release studies displayed different release pattern and hydrolysis rate analogous with PESu content. Kinetic analysis of *in vitro* release studies exhibited controlled release pattern of the drug. According to antifungal studies, mats were superior against several fungi. Penetration and permeation values of the mats were relatively negligible. Finally, histopathology examination, after PLA/PESu mats application, did not show significant skin irritation in epidermis and dermis. To conclude, the prepared formulations seem to be very promising alternative VRZ delivery systems in terms of eliminating harmful side effects in patients such as pregnant women and children.

Conflicts of interest

The authors would like to declare no conflict of interest.

Acknowledgements

The authors would like to acknowledge Istanbul Medipol University MEDITAM for enabling us to use its laboratory instruments.

References

[1] P. Siafaka, N. Üstündağ Okur, M. Mone, S. Giannakopoulou, S. Er, E. Pavlidou, E. Karavas, D. Bikiaris, Two different approaches for oral administration of Voriconazole loaded formulations: electrospun fibers versus β-cyclodextrin complexes, Int. J. Mol. Sci. 17 (2016) 282.
[2] M. Murphy, E.M. Bernard, T. Ishimaru, D. Armstrong, Activity of Voriconazole (UK-109,496) against clinical isolates of Aspergillus species and its effectiveness in an experimental model of invasive pulmonary aspergillosis, Antimicrob. Agents Chemother. 41 (1997) 696–698.
[3] H. Sanati, P. Belanger, R. Fratti, M. Ghannoum, A new triazole, Voriconazole (UK-109,496), blocks sterol biosynthesis in Candida albicans and Candida Krusei, Antimicrob. Agents Chemother. 41 (1997) 2492–2496.
[4] S.S. Kumar, R. Thakuria, A. Nangia, Pharmaceutical cocrystals and a nitrate salt of Voriconazole, CrystEngComm 16 (2014) 4722.
[5] J.D. Bos, M.L. Kapsenberg, The skin immune system its cellular constituents and their interactions, Immunol. Today 7 (1986) 235–240.
[6] E.R. Mann, K.M. Smith, D. Bernardo, H.O. Al-Hassi, S.C. Knight, A.L. Hart, Review: skin and the immune system, J. Clin. Exp. Dermatol. Res. 4 (2014) 1–16.
[7] S.-H. Kim, S.-H. Cho, S.-K. Youn, J.-S. Park, J.T. Choi, Y.-S. Bak, Y.-B. Yu, Y.K. Kim, Epidemiological characterization of skin fungal infections between the years 2006 and 2010 in Korea, Osong Public Heal. Res. Perspect. 6 (2015) 341–345.
[8] E. Kasner, C.A. Hunter, D. Ph, K. Kariko, D. Ph, Hallucinations during Voriconazole therapy, Clin. Infect. Dis. 70 (2013) 646–656.
[9] M. Shoai Tehrani, F. Sicre de Fontbrune, P. Roth, C. Allisy, M.-E. Bougnoux, O. Hermine, M. Lecuit, O. Lortholary, C. Charlier, Case report of exposure to Voriconazole in the second and third trimesters of pregnancy, Antimicrob. Agents Chemother. 57 (2013) 1094–1095.
[10] D.S. Perlin, E. Shor, Y. Zhao, Update on antifungal drug resistance, Curr. Clin. Microbiol. Rep. 2 (2015) 84–95.
[11] D. Sanglard, Emerging threats in antifungal-resistant fungal pathogens, Front. Med. 3 (2016).
[12] N.M. Mori, P. Patel, N.R. Sheth, L.V. Rathod, K.C. Ashara, Fabrication and characterization of film-forming Voriconazole transdermal spray for the treatment of fungal infection, Bull. Fac. Pharmacy Cairo Univ. 55 (2017) 41–51.
[13] A.A. Kyle, M.V. Dahl, Topical therapy for fungal infections, Am. J. Clin. Dermatol. 5 (2004) 443–451.
[14] K. Puranik, A. Tagalpallewar, Voriconazole in situ gel for ocular drug delivery, SOJ Pharm. Pharm. Sci. 2 (2015) 1–10.
[15] D. Pandurangan, P. Bodagala, V. Palanirajan, S. Govindaraj, Formulation and evaluation of Voriconazole ophthalmic solid lipid nanoparticles in situ gel, Int. J. Pharm. Investig. 6 (2016) 56–62.
[16] A. Khare, I. Singh, P. Pawar, K. Grover, Design and evaluation of Voriconazole loaded solid lipid nanoparticles for ophthalmic application, J. Drug Deliv. 2016 (2016) 1–11.
[17] R. Kumar, V.R. Sinha, Preparation and optimization of Voriconazole microemulsion for ocular delivery, Colloids Surfaces B Biointerfaces 117 (2014) 82–88.
[18] X. Sun, Z. Yu, Z. Cai, L. Yu, Y. Lv, Voriconazole composited polyvinyl alcohol/hydroxypropyl-β-cyclodextrin nanofibers for ophthalmic delivery, PLoS One 11 (2016) e0167961.
[19] Y.-H. Kim, C.K. Song, E. Jung, D.-H. Kim, D.-D. Kim, A microemulsion-based hydrogel formulation containing Voriconazole for topical skin delivery, J. Pharm. Investig. 44 (2014) 517–524.
[20] S.H. Song, K.M. Lee, J.B. Kang, S.G. Lee, M.J. Kang, Y.W. Choi, Improved skin delivery of Voriconazole with a nanostructured lipid Carrier-Based hydrogel formulation, Chem. Pharm. Bull. 62 (2014) 793–798.
[21] J.Y. Park, I.H. Lee, Controlled release of Ketoprofen from electrospun porous polylactic acid (PLA) nanofibers, J. Polym. Res. 18 (2011) 1287–1291.
[22] P.I. Siafaka, P. Barmbalexis, D.N. Bikiaris, Novel electrospun nanofibrous matrices prepared from poly(lactic acid)/poly(butylene adipate) blends for controlled release formulations of an anti-rheumatoid agent, Eur. J. Pharm. Sci. 88 (2016) 12–25.
[23] Z. Mai, J. Chen, T. He, Y. Hu, X. Dong, H. Zhang, W. Huang, F. Ko, W. Zhou, Electrospray biodegradable microcapsules loaded with curcumin for drug delivery systems with high bioactivity, RSC Adv. 7 (2017) 1724–1734.
[24] H. Zhou, A.H. Touny, S.B. Bhaduri, Fabrication of novel PLA/CDHA bionanocomposite fibers for tissue engineering applications via electrospinning, J. Mater. Sci. Mater. Med. 22 (2011) 1183–1193.
[25] M.S. Lopes, A.L. Jardini, R.M. Filho, Poly (lactic acid) production for tissue engineering applications, Procedia Eng. 42 (2012) 1402–1413.
[26] M. Santoro, S.R. Shah, J.L. Walker, A.G. Mikos, Poly(lactic acid) nanofibrous scaffolds for tissue engineering, Adv. Drug Deliv. Rev. 107 (2016) 206–212.
[27] P.I. Siafaka, P. Barmpalexis, M. Lazaridou, G.Z. Papageorgiou, E. Koutris, E. Karavas, M. Kostoglou, D.N. Bikiaris, Controlled release formulations of risperidone antipsychotic drug in novel aliphatic polyester carriers: data analysis and modelling, Eur. J. Pharm. Biopharm. 94 (2015) 473–484.
[28] Z. Qiu, M. Komura, T. Ikehara, T. Nishi, DSC and TMDSC study of melting behaviour of poly(butylene succinate) and poly(ethylene succinate), Polymer (Guildf). 44 (2003) 7781–7785.

[29] E.M. Woo, Y.-T. Hsieh, W.-T. Chen, N.-T. Kuo, L.-Y. Wang, Immiscibility-miscibility phase transformation in blends of poly(ethylene succinate) with poly(l-lactic Acid)s of different molecular weights, J. Polym. Sci. Part B Polym. Phys. 48 (2010) 1135–1147.
[30] Y. Il Yoon, K.E. Park, S.J. Lee, W.H. Park, Fabrication of microfibrous and nano-/microfibrous scaffolds: melt and hybrid electrospinning and surface modification of poly(l-lactic acid) with plasticizer, Biomed Res. Int. 2013 (2013).
[31] N. Üstündağ-Okur, A. Yoltas, V. Yozgatli, Development and characterization of Voriconazole loaded in situ gel formulations for ophthalmic application, Turkish J. Pharm. Sci. 13 (2016) 311–317.
[32] P. Siafaka, M. Betsiou, A. Tsolou, E. Angelou, B. Agianian, M. Koffa, S. Chaitidou, E. Karavas, K. Avgoustakis, D. Bikiaris, Synthesis of folate- pegylated polyester nanoparticles encapsulating ixabepilone for targeting folate receptor over-expressing breast cancer cells, J. Mater. Sci. Mater. Med. 26 (2015) 275.
[33] P.I. Siafaka, A.P. Zisi, M.K. Exindari, I.D. Karantas, D.N. Bikiaris, Porous dressings of modified chitosan with poly(2-hydroxyethyl acrylate) for topical wound delivery of levofloxacin, Carbohydr. Polym. 143 (2016) 90–99.
[34] S. Dash, P.N. Murthy, L. Nath, P. Chowdhury, Kinetic modeling on drug release from controlled drug delivery systems, Acta Pol. Pharm. 67 (2010) 217–223.
[35] B. Aksu, A. Yurdasiper, M.A. Ege, N.Ü. Okur, H. Yesim, Development and comparative evaluation of extended release indomethacin capsules, African J. Pharm. Pharmacol. 7 (2013) 2201–2209.
[36] M.A. Ege, H.Y. Karasulu, E. Karasulu, G. Ertan, A computer program designed for in vitro dissolution kinetics, in vitro-in vivo kinetic correlations and routine application, 4th Central European Symposium on Pharmaceutical Technology, Scientia Pharmaceutica Supplement 1 Band, Vienna, 2001, pp. S127–S128.
[37] J. Siepmann, N.A. Peppas, Higuchi equation: derivation, applications, use and misuse, Int. J. Pharm. 418 (2011) 6–12.
[38] R. Kharat, Mathematical models of drug dissolution: a review, Sch. Acad. J. Pharm. 3 (2014) 2320–4206.
[39] J. Crank, The mathematics of diffusion, second ed., Oxford Univ. Press, UK, 1975.
[40] P. Costa, J.M. Sousa Lobo, Modeling and comparison of dissolution profiles, Eur. J. Pharm. Sci. 13 (2001) 123–133.
[41] B. Sinha, B. Mukherjee, G. Pattnaik, Poly-lactide-co-glycolide nanoparticles containing Voriconazole for pulmonary delivery: in vitro and in vivo study, Nanomed. Nanotechnol. Biol. Med. 9 (2013) 94–104.
[42] A. Wagner, V. Poursorkhabi, A.K. Mohanty, M. Misra, Analysis of porous electrospun fibers from poly(l-lactic acid)/poly(3-hydroxybutyrate- co -3-hydroxyvalerate) blends, ACS Sustain. Chem. Eng. 2 (2014) 1976–1982.
[43] J.M. Tejashwini, P. Ashok Kumar, S.V.K., Formulation and evaluation of sustained release matrix tablets of Voriconazole using synthetic polymers, Int. J. Pharm. Res. Sch. 4 (2015) 1–18.
[44] Q. Cai, J. Bei, S. Wang, In vitro study on the drug release behavior from polylactide-based blend matrices, Polym. Adv. Technol. 13 (2002) 534–540.
[45] T. Ehtezazi, C. Washington, Controlled release of macromolecules from PLA microspheres: using porous structure topology, J. Control. Release 68 (2000) 361–372.
[46] A.I. Romero, M. Villegas, A.G. Cid, M.L. Parentis, E.E. Gonzo, J.M. Bermúdez, Validation of kinetic modeling of progesterone release from polymeric membranes, Asian J. Pharm. Sci. 13 (2017) 54–62.
[47] Y. Fu, W.J. Kao, Drug release kinetics and transport mechanisms of non-degradable and degradable polymeric delivery systems, Expert Opin. Drug Deliv. 7 (2010) 429–444.
[48] K. Frederiksen, R.H. Guy, K. Petersson, Formulation considerations in the design of topical, polymeric film-forming systems for sustained drug delivery to the skin, Eur. J. Pharm. Biopharm. 91 (2015) 9–15.
[49] D. Chantasart, P. Tocanitchart, A. Wongrakpanich, V. Teeranachaideekul, V.B. Junyaprasert, Fabrication and evaluation of eudragit® polymeric films for transdermal delivery of piroxicam, Pharm. Dev. Technol. (2017) 1–9.
[50] N. Üstündağ Okur, Ş. Apaydın, N.Ü. Karabay Yavaşoğlu, A. Yavaşoğlu, H.Y. Karasulu, Evaluation of skin permeation and anti-inflammatory and analgesic effects of new naproxen microemulsion formulations, Int. J. Pharm. 416 (2011) 136–144.
[51] K. Ho, T. Cheng, Common superficial fungal infections – a short review, Med. Bull. 15 (2010) 23–27.
[52] H. Jenkinson, L. Douglas, J. Interactions between Candida species and bacteria in mixed infections, in: K.A. Brogden, J.M. Guthmiller (Eds.), Polymicrobial Diseases, ASM Press, Washington DC, 2002.
[53] A. Raz-Pasteur, Y. Ullmann, I. Berdicevsky, The pathogenesis of *Candida* infections in a human skin model: scanning electron microscope observations, ISRN Dermatol. 2011 (2011) 1–6.
[54] R.J. Kothavade, M.M. Kura, A.G. Valand, M.H. Panthaki, Candida Tropicalis: its prevalence, pathogenicity and increasing resistance to fluconazole, J. Med. Microbiol. 59 (2010) 873–880.
[55] M. Isaac, Cutaneous aspergillosis, Dermatol. Clin. 14 (1996) 137–140.
[56] J.A. van Burik, R. Colven, D.H. Spach, Cutaneous aspergillosis, J. Clin. Microbiol. 36 (1998) 3115–3121.
[57] E. Abd, S. Yousuf, M. Pastore, K. Telaprolu, Y. Mohammed, S. Namjoshi, J. Grice, M. Roberts, Skin models for the testing of transdermal drugs, Clin. Pharmacol. Adv. Appl. 8 (2016) 163–176.
[58] B. Pilmis, V. Jullien, J. Sobel, M. Lecuit, O. Lortholary, C. Charlier, Antifungal drugs during pregnancy: an updated review, J. Antimicrob. Chemother. 70 (2015) 14–22.
[59] T.M. Hohl, Overview of vertebrate animal models of fungal infection, J. Immunol. Meth. 410 (2014) 100–112.
[60] K. Szalai, T. Kopp, A. Lukschal, C. Stremnitzer, J. Wallmann, P. Starkl, L. Vander Elst, J.-M. Saint-Remy, I. Pali-Schöll, E. Jensen-Jarolim, Establishing an allergic eczema model employing recombinant House dust mite allergens der P 1 and der P 2 in BALB/c mice, Exp. Dermatol. 21 (2012) 842–846.
[61] S.P. Stratton, J.L. Bangert, D.S. Alberts, R.T. Dorr, Dermal toxicity of topical (-) Epigallocatechin-3-Gallate in BALB/c and SKH1 mice, Cancer Lett. 158 (2000) 47–52.
[62] B.C. Martel, P. Lovato, W. Bäumer, T. Olivry, Translational animal models of atopic dermatitis for preclinical studies, Yale J. Biol. Med. 90 (2017) 389–402.
[63] A. Baldo, M. Monod, A. Mathy, L. Cambier, E.T. Bagut, V. Defaweux, F. Symoens, N. Antoine, B. Mignon, Mechanisms of skin adherence and invasion by dermatophytes, Mycoses 55 (2012) 218–223.